# Theoretical Studies of the ATP Hydrolysis Mechanism of Myosin

Noriaki Okimoto,* Kazunori Yamanaka,† Junko Ueno,† Masayuki Hata,† Tyuji Hoshino,† and Minoru Tsuda†
*Computational Science Laboratory, Institute of Physical and Chemical Research (RIKEN), Wako-shi, Saitama, 351-0198, Japan and †Laboratory of Physical Chemistry, Faculty of Pharmaceutical Sciences, Chiba University, Inage-ku, Chiba 263-8522, Japan

ABSTRACT The ATP hydrolysis mechanism of myosin was studied using quantum chemical (QM) and molecular dynamics calculations. The initial model compound for QM calculations was constructed on the basis of the energy-minimized structure of the myosin(S1dc)-ATP complex, which was determined by molecular mechanics calculations. The result of QM calculations suggested that the ATP hydrolysis mechanism of myosin consists of a single elementary reaction in which a water molecule nucleophilically attacked $\gamma$-phosphorus of ATP. In addition, we performed molecular dynamics simulations of the initial and final states of the ATP hydrolysis reaction, that is, the myosin-ATP and myosin-ADP·Pi complexes. These calculations revealed roles of several amino acid residues (Lys185, Thr186, Ser237, Arg238, and Glu459) in the ATPase pocket. Lys185 maintains the conformation of $\beta$- and $\gamma$-phosphate groups of ATP by forming the hydrogen bonds. Thr186 and Ser237 are coordinated to a $Mg^{2+}$ ion, which interacts with the phosphates of ATP and therefore contributes to the stabilization of the ATP structure. Arg238 and Glu459, which consisted of the gate of the ATPase pocket, retain the water molecule acting on the hydrolysis at the appropriate position for initiating the hydrolysis.

## INTRODUCTION

Myosins are molecular motors that track along actin filaments through the hydrolysis of ATP and play an important role in diverse biological contractile events. Recently, the three-dimensional structures of myosins have been determined by x-ray crystallography (Rayment et al., 1993; Fisher et al., 1995; Smith and Rayment, 1996; Gulick et al., 1997). These structural data indicated that nucleotide (ATP or ADP)- and actin-binding sites were located in the globular head of myosin, called subfragment 1 or S1.

In *Dictyostelium* myosin II (S1dc), the nucleotide-binding site (called the ATPase pocket) is surrounded by three loop structures; the P-loop (residues 179–186), the switch I loop (residues 233–240), and the switch II loop (residues 454–459). The ATPase pocket has a gate for release of phosphate, a product of ATP hydrolysis. This gate is closed or opened with the formation or disappearance of ionic bonds between the side chains of Arg238 (in the switch I loop) and Glu459 (in the switch II loop). Determination of the crystal structures of S1dc with several nucleotides and its analogs (Fisher et al., 1995; Smith and Rayment., 1996; Gulick et al., 1997) revealed that the switch I loop undergoes a minor conformational change and that the switch II loop undergoes a large conformational change. In the structures of S1dc with MgADP/BeFx, MgAMPPNP, MgATP$\gamma$S, or MgADP, the switch II loop moved away from the ATPase pocket, so that the gate was opened with the disappearance of ionic bonds. In contrast, the structures of the S1dc with MgADP/VO4 or MgADP/AlFx indicated that Arg238 formed ionic bonds with Glu459 and, consequently, the gate was closed. From analysis of these crystal structures, Rayment et al. (1993) suggested that the conformation observed in the structure of S1dc with MgADP/VO4 (Fisher et al., 1995), where the gate was closed, was necessary for the hydrolysis of ATP. In addition, many experiments on site-directed mutation of myosin have suggested that several amino acid residues of the ATPase pocket play an important role in the hydrolysis of ATP (Sasaki and Sutoh, 1998; Li et al., 1998; Furch et al., 1999; Onishi et al., 1998). From these studies, it was revealed that Lys185, Arg238, and Glu459 were closely related with the hydrolysis of ATP. It is also known that ionic bonds between Arg238 (in the switch I loop) and Glu459 (in the switch II loop) are required to support efficient ATP hydrolysis.

According to the suggestion by Bagshaw et al. (1974), the mechanism of the binding and hydrolysis of ATP by myosin consists of seven steps as shown in scheme 1, where M is myosin and Pi is a phosphate. The asterisks refer to different conformational states as detected by intrinsic protein fluorescence.

$$\mathrm{M + ATP \leftrightarrow M - ATP \leftrightarrow M^{*} - ATP \leftrightarrow M^{**}}$$
$$\mathrm{- ADP\text{-}Pi \leftrightarrow M^{*} - ADP - Pi \leftrightarrow Pi + M^{*} - ADP}$$
$$\mathrm{\leftrightarrow M - ADP \leftrightarrow M + ADP} \qquad \text{(Scheme 1)}$$

The first step is the formation of myosin with an ATP complex. The binding of ATP then induces the conformational change in the second step. In the third step, hydrolysis of ATP occurs. The fourth step is the conformational change for the release of a phosphate Pi. After the release of Pi in the fifth step, myosin with ADP complex is formed in the sixth step, and then the conformational state of myosin returns to its original state in the seventh step.

*Received for publication 29 September 2000 and in final form 31 July 2001.*

Address reprint requests to Dr. Noriaki Okiomoto, Institute of Physical and Chemical Research (RIKEN), Computational Science Laboratory, 2–1 Hirosawa, Wako-shi, Saitama, 351-0198, Japan. Tel.: 81-48-467-9417; Fax: 81-48-467-4078; E-mail: okimoto@atlas.riken.go.jp.



0006-3495/01/11/2786/09 $2.00

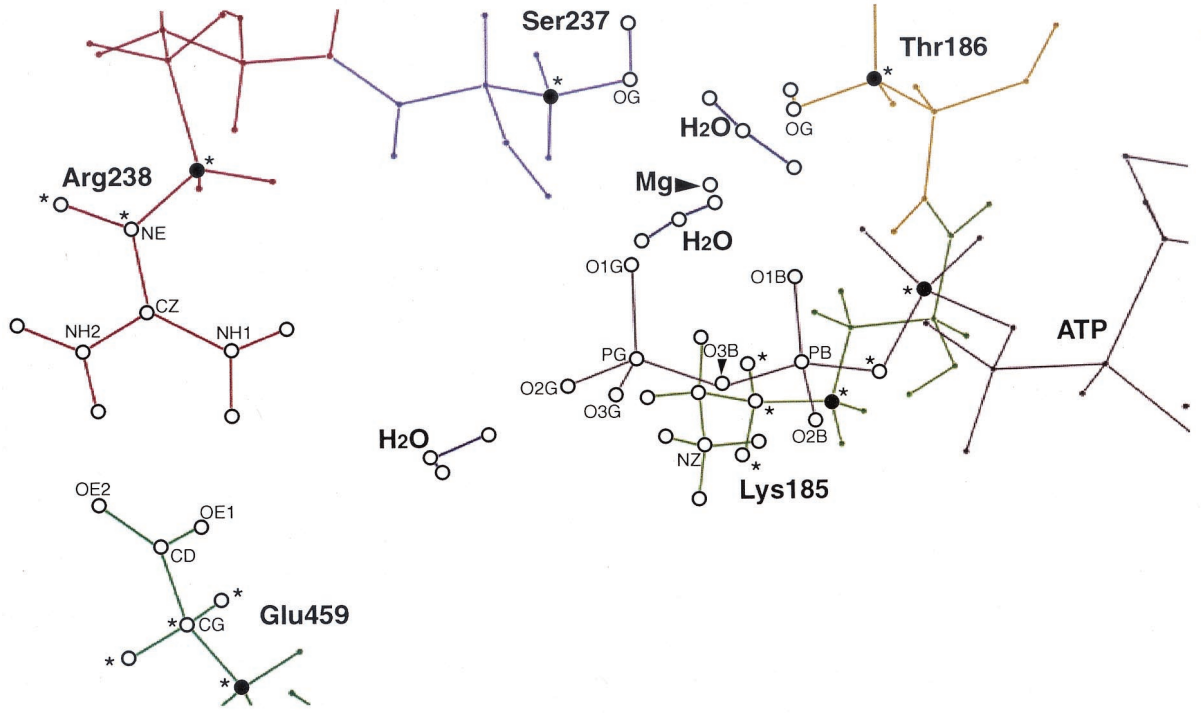


FIGURE 1 ATPase pocket in the MM-minimized structure for the myosin-ATP complex.

Based on the results of the aforementioned studies on x-ray crystallography and the site-directed mutation, we speculated that the ionic bonds between Arg238 and Glu459 were formed immediately before the hydrolysis of ATP (corresponding to the initial state of the third step in Scheme 1). The ATP hydrolysis in third step would be the core process in the sequence of Scheme 1 and has attracted the interest of many researchers. The detailed mechanism of ATP hydrolysis is, however, still unclear. In this study, we clarified the atomic-level reaction mechanism of the ATP hydrolysis by myosin using quantum chemical (QM) calculations and molecular dynamics (MD) simulations, and we examined the compatibility of our results with other experimental results.

## MATERIALS AND METHODS

### QM calculations

#### *Construction of a model compound*

For QM calculations of the ATP-hydrolysis mechanism, we used a model compound based on the energy-minimized structure of the myosin-ATP complex by molecular mechanics (MM) calculations (see MD simulation). Focusing on $\beta$- and $\gamma$-phosphates, the model compound was constructed by extracting solid- and open-circle atoms from the MM-minimized structure shown in Fig. 1 and replacing open-circle atoms with hydrogen atoms. The positions of asterisked atoms were fixed during geometry optimization because these constraints prevented the corruption of the basic structure of myosin. This model compound consists of $\beta$- and $\gamma$-phosphate groups of ATP, a $Mg^{2+}$ ion, a water molecule acting on the hydrolysis, $CH_3CH_2NH_3^+$ for Lys185, $CH_3C(NH_2)_2^+$ for Arg238, $CH_3COO^-$ for Glu459, two water molecules for Thr186 and Ser237 that interact with the $Mg^{2+}$ ion, and two water molecules coordinating to the $Mg^{2+}$ ion. A schematic representation of the model compound is shown in Fig. 2.

#### *Computational details*

The Schrödinger equation of the model compound was solved by the Hartree-Fock method using the 6–31G** basis set (Szabo and Ostlund, 1989). The model structures at the minimum points and transition states (TS) on the potential energy hypersurface were fully optimized using the

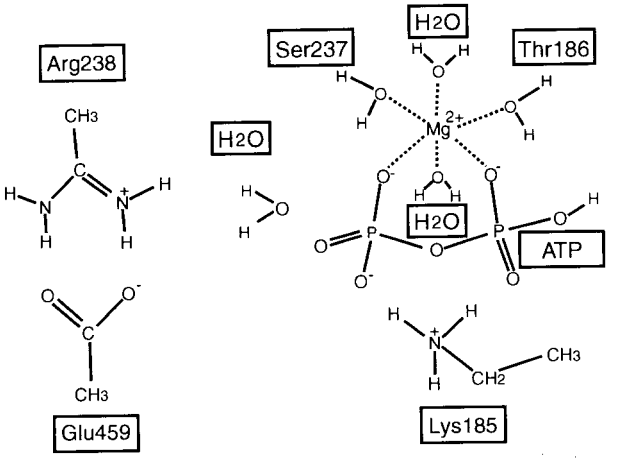


FIGURE 2 Initial model compound for QM calculations.

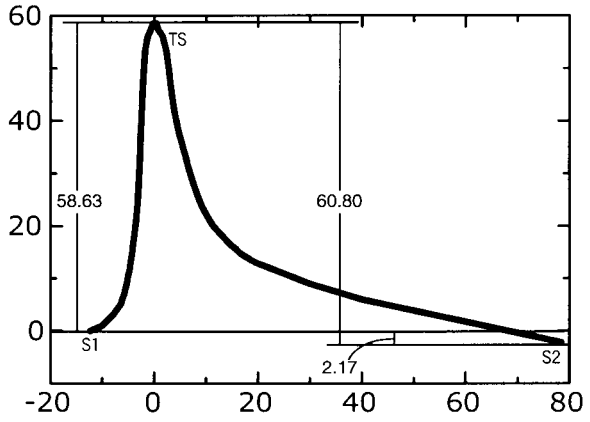


FIGURE 3 Total potential energy curve for ATP hydrolysis. The ordinate is the potential energy differences (kcal/mol) and the abscissa is the intrinsic reaction coordinate (amu$^{1/2}$ Å).

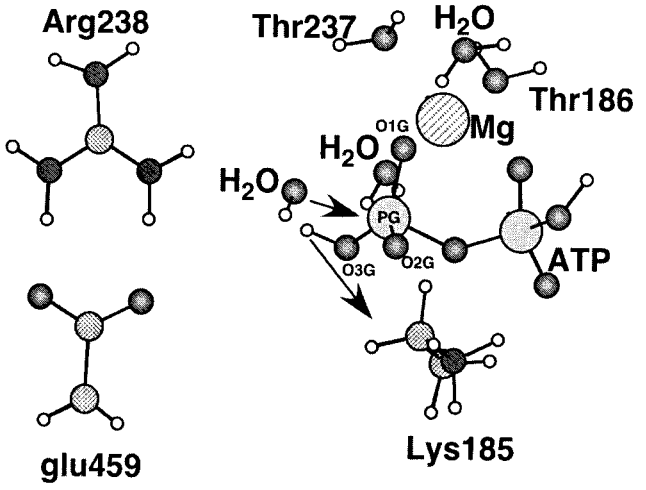


FIGURE 4 Normal vibrational mode of the imaginary frequency of the structure of each TS that appears in the hydrolysis. The arrows indicate the forward direction of the ATP hydrolysis.

energy gradient method. Frequency analysis of the structure of the TS indicated the presence of an imaginary frequency. The lowest energy reaction path was determined by calculating the steepest descent paths from each TS in both the forward and reverse directions following the normal vibrational mode of the imaginary frequency. The structures of a reactant and a product connected to the TS resulted from this calculation. The intrinsic reaction coordinate in Fig. 3 represents the lowest energy reaction path expressed in mass-weighted coordinates. For checking the reliability of potential energy, we carried out calculations by the density functional theory method using Becke's three-parameter hybrid method (Becke, 1993) and using LYP correlation functions (B3LYP) (Lee et al., 1988; Miehlich et al., 1989) on the structures of the stable and TS which were determined at HF/6–31G**. The computational program used was Gaussian 98 (Frisch et al., 1998).

## MD simulations

### *Construction of the initial structure*

We carried out MD simulations of myosin-ATP and myosin-ADP·Pi complexes, which are the initial and final states of ATP hydrolysis. The initial structures of these complexes were constructed on the basis of the x-ray crystallographic structure of the myosin-ADP/VO4 complex (code in Protein Data Bank (Abola et al., 1987, 1996; Bernstein et al., 1977): 1VOM (Smith and Rayment, 1996)). Because many amino acid residues were not determined in the coordinate data of this x-ray crystal structure, we repaired these amino acid residues (Ala205-Ser208, Asn711, Ala716-Ser719, and Asp724-Leu730) by using a homology module of Insight II (Insight II, version 95.0, Molecular Simulations Inc., San Diego). The N-terminal amino acid residue, Met1, of myosin (S1dc) was also not determined because of its flexibility, and we therefore added it to the S1dc. Thus, the myosin (S1dc) structure for MD simulations was constructed of 747 amino acid residues. The structure of ATP was made by shortening the distance between the vanadium atom of the vanadate $VO_4$ and the oxygen atom of $\beta$-phosphate to a normal P-O bond distance and replacing the vanadium atom with a phosphorus atom. A water molecule acting on the hydrolysis (lytic water molecule) was generated on the basis of the position of the oxygen atom that had the longest V-O bond among the four V-O bonds. The structures of ADP and phosphate Pi were determined on the basis of the results of QM calculations (see Results). We determined the parameters of ATP, ADP, and Pi by QM calculations using the Hartree-Fock method/6–31G* basis set.

### *Calculations*

MM potential energy minimizations and MD simulations were carried out using the program package AMBER (version 5.0, University of California) (Pearlman et al., 1995). Calculations were performed using an all-atom force field of Cornell et al., (1995). The system was solvated in a rectangular box of ~108 Å × 85 Å × 76 Å in size, and 20,240 TIP3P water molecules (Jorgensen et al., 1983) were generated in the box. The periodic boundary condition was applied and the pressure was kept constant in the system. The temperature was kept constant according to Berendsen' s algorithm with a coupling time of 0.2 ps (Berendsen et al., 1984). To simplify this calculation, the SHAKE method was used (Ryckaert et al., 1977). The nonbonded interactions were calculated by the dual cutoff method. The distance of the first cutoff was 12 Å and that of the second cutoff was 15 Å. The integration time step of the MD simulations was 1 fs.

The strategy of our simulations was as follows. First, potential energy minimizations were performed on the initial systems. In the potential energy minimization, the steepest descent method was used for the early cycles and then the conjugate gradient method was used later. The minimized structure of the myosin-ATP complex was used for the construction of the model compound for QM calculations, as described before. Next, MD simulations were performed on the energy-minimized systems, taking careful consideration of the temperature setting. After 10-ps MD simulations at 300 K only for the solvent water molecules with the enzyme, nucleotide, and crystal water molecules fixed, the temperature of all systems was gradually increased by heating to 300 K for the first 60 ps, and then it was kept at 300 K for the next 500 ps. The trajectories at this temperature (300 K for 500 ps) were considered to be the most probable structure under physiologic conditions and were analyzed in detail.

## RESULTS

### QM calculation: analysis of potential energy

As seen in the potential energy curve (Fig. 3), QM calculations at HF/6–31G** revealed that a single elementary reaction comprised the mechanism of ATP hydrolysis. We determined the structure of the TS from the initial model compound. Fig. 4 shows the unique imaginary frequency of the structure of this TS. The normal vibrational mode of the

**TABLE 1 Total potential energy values for ATP hydrolysis obtained by Hartree-Fock and DFT methods**

| Method/Basis set | S1 | TS | S2 |
|---|---|---|---|
| HF/6-31G** | 0 | 58.63 | −2.17 |
| B3LYP/6-31G** | 0 | 41.97 | −6.19 |

Values indicate potential energy in kcal/mol.

imaginary frequency indicated that the oxygen and hydrogen atoms of the water molecule combined with the phosphorus and oxygen atoms of the γ-phosphate, respectively. The potential energy drop along the steepest descendent path in the forward direction of the hydrolysis reaction transformed the TS into the final state, S2, the product of the hydrolysis. In contrast, the potential energy drop in the opposite direction led to the initial state of the hydrolysis reaction, S1 (Fig. 3). The hydrolysis reaction required an activation energy of 58.63 kcal/mol, and the potential energy of S2 was 2.17 kcal/mol lower than that of S1. For more exact analysis of energy, we calculated the potential energies of S1, TS, and S2 by the density functional theory method. The results are shown in Table 1. QM calculations at B3LYP/6–31G** revealed that its activation energy was 41.97 kcal/mol, which was lower than that of HF/6–31G** by ~17 kcal/mol. The potential energy of S2 was more stable than that of S1 by 6.19 kcal/mol.

## QM calculations: analysis of structures

The structures of the stable states (S1, S2) and the TS that appeared in the hydrolysis reaction are shown in Fig. 5.

The initial state of hydrolysis, S1, was the myosin-ATP complex (see Fig. 5, S1). In the structure of S1, a lytic water molecule was between the gate of the ATPase pocket (Arg238 and Glu459) and the γ-phosphate of ATP. The distance between the water molecule and γ-phosphate was 3.41 Å; thus, there is an effective interaction to initiate the hydrolysis reaction. This water molecule formed a hydrogen bond with Arg238 rather than with Glu459. At this time, the $Mg^{2+}$ ion was surrounded by six ligands in an octahedral arrangement. The $Mg^{2+}$ ion interacted with oxygen atoms O1B and O1G of β- and γ-phosphate in ATP and therefore contributed to maintenance of the appropriate conformation of phosphates in the ATPase pocket. The OG atom of

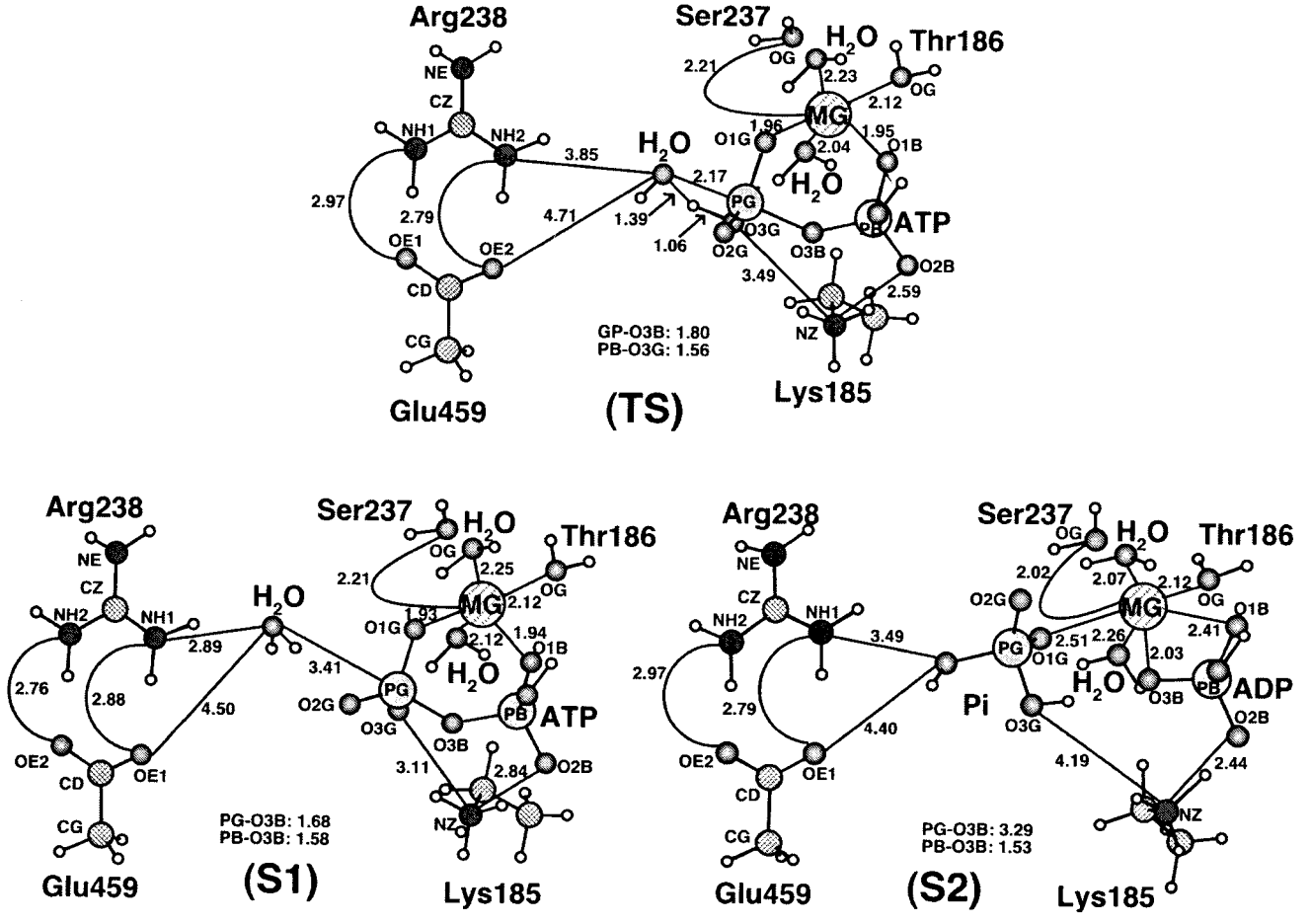


FIGURE 5 Structures of the stable states (S1 and S2) and the TS that appear in the hydrolysis. Numbers are the interatomic distances in Å.

Thr186, the OG atom of Ser237, and two water molecules were also coordinated to the $Mg^{2+}$ ion. Lys185 formed two hydrogen bonds with the O3G and O2B atoms of γ- and β-phosphates (O3G(ATP)-NZ(Lys185): 3.11 Å, O2B (ATP)-NZ(Lys185): 2.84 Å), so that the conformation of γ-phosphate was maintained in the ATPase pocket.

The TS structure appeared when the oxygen atom of the lytic water molecule approached the phosphorus atom PG of the γ-phosphate (see Fig. 5, PG(γ-phosphate)-O(water): 2.17 Å). At this time, the hydrogen atom was just in the process of transferring to the oxygen atom O3G of the γ-phosphate. The movement of the hydrogen atom increased the distance between the O3G atom of γ-phosphate and the NZ atom of Lys185.

The final state of the hydrolysis, S2, was the myosin-ADP·Pi complex (see Fig. 5, S2). In this structure, the OH group from the lytic water molecule was linked to the PG atom of the γ-phosphate, and the hydrogen atom initially attached to the water molecule transferred completely to the O3G atom of γ-phosphate. These movements resulted in dissociation of phosphate Pi from the ATP molecule. At this time, the distance between β-phosphate and Pi was 3.29 Å. This dissociation caused the disappearance of the hydrogen bond between the O3G atom of Pi and the NZ atom of Lys185 and the formation of a stronger hydrogen bond (low-barrier hydrogen bond) between the O2B atom of β-phosphate and the NZ atom of Lys185. The Pi was moved from the nucleotide (ADP) and approached the gate of the ATPase pocket. The conformation of ligands interacting with the $Mg^{2+}$ ion was different from that of the S1 structure. The structure of β-phosphate was changed by the dissociation of Pi from ATP, so that the interaction between O3B and $Mg^{2+}$ atoms became stronger, whereas the interaction between O1B and $Mg^{2+}$ atoms became a little weaker. The interaction between O1G and $Mg^{2+}$ atoms also became weaker.

Fig. 6 shows an interesting feature of the structural change in this ATP hydrolysis mechanism. The dihedral angle O1G-O2G-O3G-PG of γ-phosphate was 28.37° in S1, 9.94° in TS, and −33.04° in S2. Information on the dihedral angles indicated that inversion of the γ-phosphate occurs. As shown in Fig. 5, a lytic water molecule approached the PG atom on a PG-O3B bond line. This fact revealed that a Walden inversion reaction occurs in ATP hydrolysis.

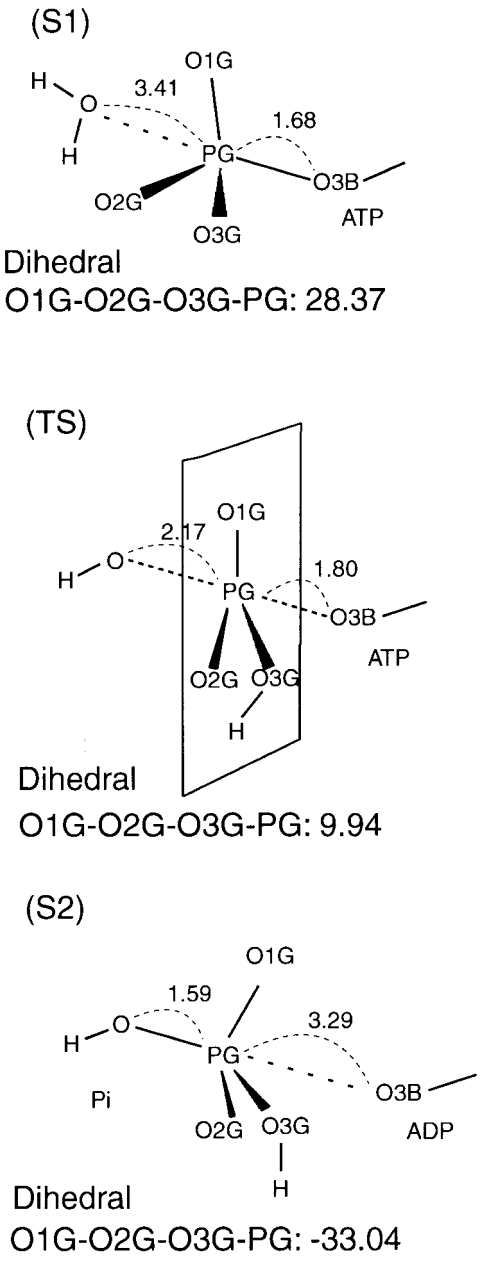


FIGURE 6 Structural change in γ-phosphate in the ATP hydrolysis mechanism. The dihedral angles O1G-O2G-O3G-PG of γ-phosphate were 28.37° in S1, 9. 94° in TS, and −33.04° in S2.

## MD simulations of myosin-ATP and myosin-ADP·Pi complexes

MD simulations were carried out for both myosin-ATP and myosin-ADP·Pi complexes. Figs. 7 and 8 show the average structures of these two complexes.

In the average structure of the myosin-ATP complex (Fig. 7), a lytic water molecule existed between the gate of the ATPase pocket (Arg238 and Glu459) and γ-phosphate of ATP, as in the S1 structure determined by QM calculations. The distance between the lytic water molecule and γ-phosphate was 3.30 Å, similar to the value obtained by QM calculations (3.41 Å). However, the distance between the lytic water molecule and Arg238 was 3.79 Å, which is longer by 0.9 Å than the value of the S1 structure. The reason for this difference would be that the model compound for the QM calculations does not take Gly457 into consideration. In the MD simulation, the main chain NH group of Gly457 formed a hydrogen bond with this lytic water molecule. By this hydrogen bond, the position of the

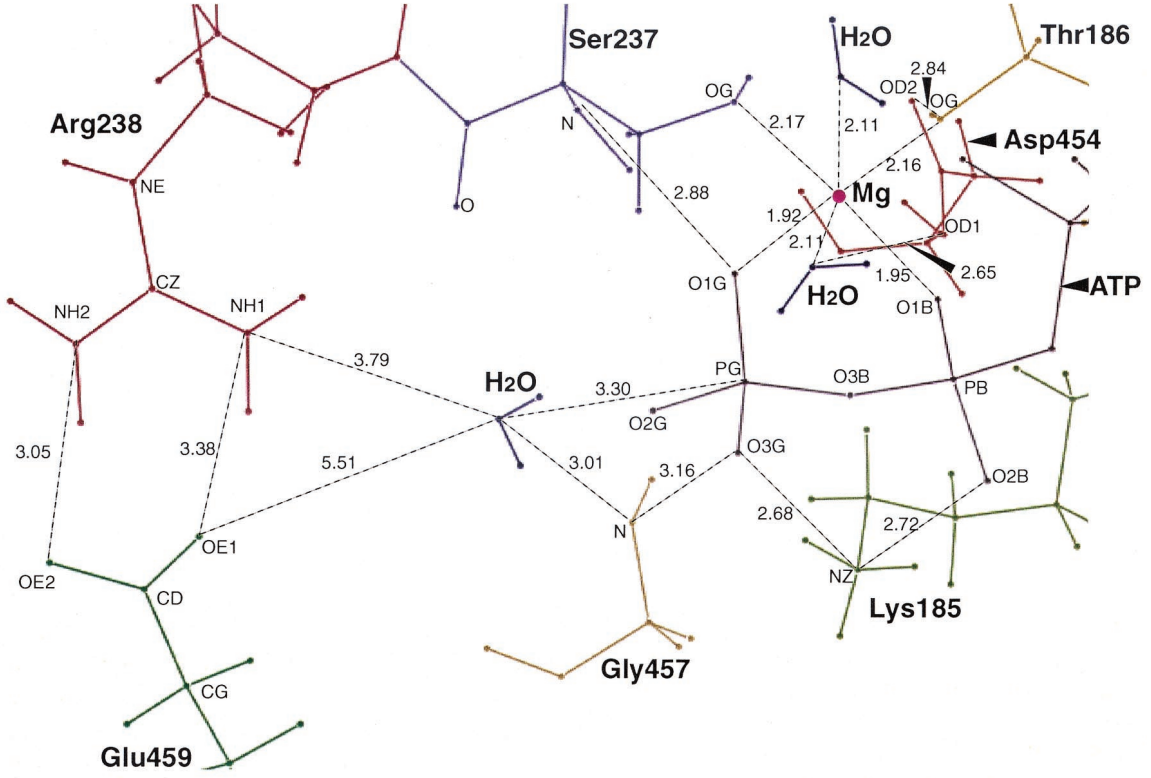


FIGURE 7 Average structure for 500-ps MD simulation for the myosin-ATP complex. Numbers are the interatomic distances in Å.

lytic water molecule was closer to ATP than that of the S1 structure. In the same manner as that of the of S1 structure, the NZ atom of Lys185 formed hydrogen bonds with O3G and O2B atoms and helped to maintain the conformation of the $\beta$- and $\gamma$-phosphates in the ATPase pocket. The conformation involving the $Mg^{2+}$ ion is similar to the crystal structures and the results of QM calculations. The $Mg^{2+}$ ion interacts with six ligands (Thr186, Ser237, $\gamma$- and $\beta$-phosphates, and two water molecules). The side chain of Asp454 faced the ATPase pocket and formed hydrogen bonds with Thr186 and the water molecule, but Asp454 did not directly interact with the $Mg^{2+}$ ion. In these aspects, the results of MD simulation of the myosin-ATP complex almost accorded with the results of QM calculations.

The results of MD simulation of the myosin-ADP·Pi complex are as follows. In the MD simulation (Fig. 8), the dissociating Pi formed hydrogen bonds with the NZ atom of Lys185, N and O atoms of Ser237, and the N atom of Gly457, and it was therefore maintained stably in the ATPase pocket. The hydrogen bond between the NZ atom of Lys185 and the O2B atom of $\beta$-phosphate was maintained during the simulation, in the same way as that of the S2 structure. The conformation of the ligands involving the $Mg^{2+}$ ion was similar to the results of QM calculations; namely, the $Mg^{2+}$ ion interacted with the oxygen atom (O3B atom) of $\beta$-phosphate in addition to the six ligands observed in MD simulation of the myosin-ATP complex.

## MD simulation of myosin-ATP complex in the mutation of G457A or D454A

In our QM calculations, Gly457 and Asp454 were not included in the model compounds. Some experimental study with mutation technique suggested that these amino residues, Gly457 and Asp454, had a relation to the activity of ATP hydrolysis as well as Lys185, Arg238, and Glu459 (Sasaki and Sutoh, 1998). Accordingly, MD simulations were also performed for two mutants, G457A and D454A, to examine the involvement of these residues in ATPase activity. The MD computational method was the same as the previous section.

Table 2 shows the average interatomic distances during the 500-ps MD simulations at 300 K for three types of myosin-ATP complexes (wild, G457A, and D454A). No prominent conformational differences are seen among the three. In the simulation of G457A, the distance between the NH1 atom of Arg238 and lytic water increased by 0.7 Å compared with the wild-type. This is attributed to the absence of the hydrogen bond between the O3G atom of ATP and the N atom of Ala457. The G457A mutation caused the steric hindrance of the side chain of alanine and the N atom of Gly457 could make a hydrogen bond only with the lytic water. In the wild-type, the N atom of Gly457 has two hydrogen bonds with the lytic water and the O3G atom of ATP. Hence, the position of the lytic water was

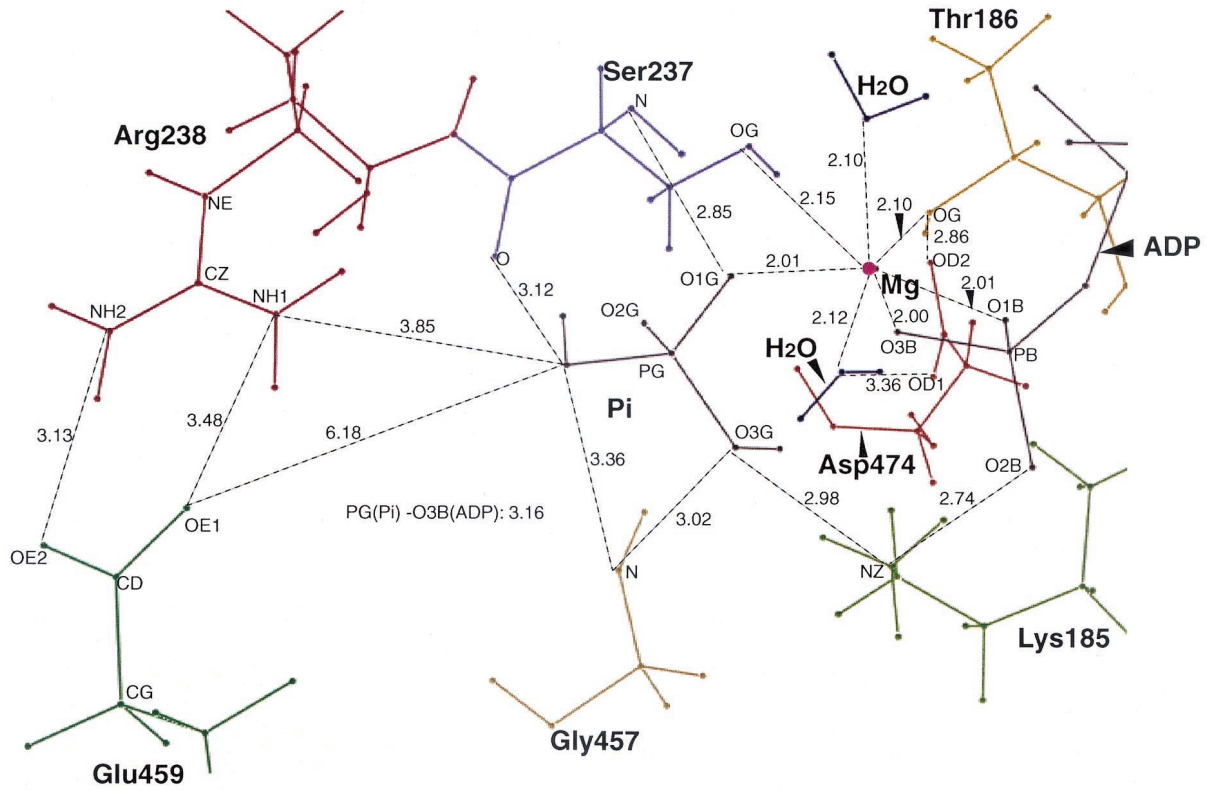


FIGURE 8 Average structure for 500-ps MD simulation for the myosin-ADP·Pi complex. Numbers are the interatomic distances in Å.

shifted toward ATP. No other obvious difference in interatomic distances between wild-type and G457A is seen in Table 2.

In the simulation of D454A, most interatomic distances are consistent between wild-type and D454A mutant with the exception of the OE1 atom of Glu459, the O atom of lytic water. Because Glu459 is located at the opposite position to Asp454, the D454A mutation seems not to be a direct reason for the change of the OE1 atom of Glu459, the O atom of lytic water distance.

Despite an experimental suggestion of low activity of ATP hydrolysis in the G457A and D454A mutants, the present MD simulation did not demonstrate any significant difference between wild-type myosin and those mutants. In the section QM calculations: analysis of structures, the QM calculation could give a reaction path of ATP hydrolysis without those amino residues. Consequently, it would be concluded that Gly457 and Asp454 had a minor role for the ATP → ADP conversion reaction. We speculate that a low ATPase activity in G457A and D454A mutant is attributable to other reasons, such as problems in incorporating ATP or water at the catalytic site.

## DISCUSSION

Our QM calculations revealed that the mechanism of ATP hydrolysis by myosin was a single elementary reaction accompanied by Walden inversion of γ-phosphate. This result explained the outline of the mechanism. In addition to the information obtained by QM calculations, MD simulations clarified the effects of many amino acid residues in the ATPase pocket. We show the roles of the amino acid residues in the ATPase pocket by analyzing our computational results.

From QM and MD calculations of the myosin-ATP complex (see Figs. 5 (S1) and 7), Lys185 prevents the deformation of the β- and γ-phosphates of ATP by forming hydrogen bonds with O3G and O2B atoms, and it plays a role in maintaining the appropriate structure of ATP for generation of hydrolysis. In MD simulation of the myosin-ADP·Pi complex (Fig. 8), Lys185 formed hydrogen bonds with the O3G atom of Pi and the O2B atom of β-phosphate in ADP and contributed to the stabilization of myosin-ADP·Pi complex structure, which seemed to be in a semistable state. This lysine commonly exists in kinesin and G-protein, each of which has the activity of ATP or GTP hydrolysis. Studies on their crystal structures indicated that lysine played a common role in these proteins because the similar hydrogen bonds involving lysine were formed. In our QM calculations, because the distances between the NZ atom of Lys185 and the O3G atom of γ-phosphate in S1, TS, and S2 structures are 3.11, 3.49, and 4.19 Å, respectively, the hydrogen bond must have been lost with the progress of the reaction. In S1, the NZ atom of Lys185

**TABLE 2 Comparison of interatomic distances between wild-type ATP-bound myosin and G457A and D454A mutants**

| | Wild | G457A | D454A |
|---|---|---|---|
| Arg238 NH1-Glu459 OE1 | 3.38 | 2.81 | 2.79 |
| Arg238 NH2-Glu459 OE2 | 3.05 | 2.89 | 2.96 |
| Arg238 NH1-lytic water | 3.79 | 4.45 | 3.27 |
| Glu459 OE1-lytic water | 5.51 | 5.46 | 4.53 |
| Gly457 N-lytic water | 3.01 | | 3.01 |
| Ala457 N-lytic water | | 2.97 | |
| ATP PG-lytic water | 3.30 | 3.26 | 3.33 |
| ATP O3G-Gly457 N | 3.16 | | 3.42 |
| ATP O3G-Ala457 N | | 4.42 | |
| ATP O3G-Lys185 NZ | 2.68 | 2.66 | 2.67 |
| ATP O1G-Ser237 N | 2.88 | 2.86 | 2.78 |
| ATP O2G-Lys185 NZ | 2.72 | 2.72 | 2.71 |
| Mg-ATP O1G | 1.92 | 1.92 | 1.92 |
| Mg-ATP O1B | 1.95 | 1.95 | 1.95 |
| Mg-Ser237 OG | 2.17 | 2.19 | 2.19 |
| Mg-Thr186 OG | 2.16 | 2.12 | 2.13 |
| Mg-water A* | 2.11 | 2.10 | 2.15 |
| Mg-water B* | 2.11 | 2.13 | 2.09 |
| Asp 454 OD1-water B* | 2.65 | 3.67 | |
| Asp454 OD2-Thr186 OG | 2.84 | 2.07 | |

*On two water molecules interacting with the $Mg^{2+}$ ion, water B corresponds to the water near Asp454, and the other is water A.
Values are time average during 500-ps MD simulations at 300 K.

formed a hydrogen bond with the O3G atom, and then the O3G atom acted as a proton acceptor for a lytic water molecule, and, as a consequence, the hydrogen bond was lost. In contrast, this hydrogen bond was maintained in the MD simulation of the myosin-ADP·Pi complex because the O3G atom of Pi was maintained by the formation of many hydrogen bonds with amino acid residues in the ATPase pocket. These results suggest that the reason why K185Q mutant myosin did not exhibit ATPase activity (Li et al., 1998), in which Gln185 was not able to form hydrogen bonds with $\beta$- and $\gamma$-phosphate, and thus the structure of $\beta$- and $\gamma$-phosphates was deformed and the lytic water molecule could not attack the $\gamma$-phosphate. From this point, it is thought that Lys185 plays a role in maintaining the appropriate structure of phosphate groups in the nucleotide.

Thr186 and Ser237 are coordinated to the $Mg^{2+}$ ion, which interacts strongly with the $\beta$- and $\gamma$-phosphates of the nucleotide in QM and MD calculations. These two amino acid residues maintain the conformation of these phosphates of the nucleotide through the $Mg^{2+}$ ion. According to the results of an experiment on site-directed mutation (Sasaki and Sutoh., 1998), S237A mutant myosin exhibited a low ATPase activity. We speculate that the disappearance of the hydroxy group because of the replacement of alanine causes a change in the conformation involving the $Mg^{2+}$ ion, thus preventing the occurrence of ATP hydrolysis. In the myosin-ATP complex, six ligands were coordinated to the $Mg^{2+}$ ion in good balance, and the structure of $\gamma$-phosphate became suitable for ATP hydrolysis. Thus, Thr186 and Ser237 are important amino acid residues.

We describe below the roles of Arg238 and Glu459, which comprise the gate of the ATPase pocket. The results of QM and MD calculations showed that Arg238 and Glu459 formed ionic bonds with one another during the process of ATP hydrolysis. In the S1 structure (Fig. 5), Arg238 formed a hydrogen bond with a lytic water molecule (water molecule-Arg238: 2.89 Å). MD simulation of the myosin-ATP complex revealed that the distance between a lytic water molecule and Arg238 was long enough for initiation of the hydrolysis, although the effect of the other amino acid residues containing Gly457 increased the distance to 3.79 Å. It is interesting that the oxygen of the lytic water molecule faces toward the opposite direction of the nucleophilic attack on $\gamma$-phosphorus of ATP. This is why Arg238 acts as a proton donor. According to the experimental data of R238E/E459R double mutant myosin, the ATPase activity of this mutant myosin was equal to that of the wild-type myosin (Furch et al., 1999). This suggests that the ATPase hydrolysis does not depend on the orientation of the water molecule. Arg238 plays a role in maintaining the appropriate position of the water molecule for ATP hydrolysis. However, it is thought that Glu459 did not directly contribute to the dissociation reaction of ATP (Figs. 5, 7, and 8), though it formed ionic bonds with Arg238. The results of our calculations revealed that the distance between a lytic water molecule and Glu459 was $\sim$5 Å, and there was therefore not a sufficient interaction. In addition, Glu459 formed ionic bonds with Arg238 during ATP hydrolysis. Therefore, it is unlikely that Glu459 acts as a base in the hydrolysis. However, we believe that Glu459 plays a role in the opening and closing of the ATPase pocket and in the capture of a lytic water molecule acting on the hydrolysis. Experiments on site-directed mutation of Arg238 and Glu459 (Sasaki and Sutoh, 1998; Li et al., 1998; Furch et al., 1999; Onishi et al., 1998) showed that substitution of Ile, Ala, or Glu for Arg causes a decrease in ATPase activity, and that the substitution of Arg or Ala for Glu also causes a decrease in ATPase activity. However, ATPase activity of R238K mutant myosin was very similar to that of the wild-type myosin (Li et al., 1998). Furthermore, the double substitutions of Glu and Arg for Arg and Glu exhibited the same ATPase activity as that of wild-type myosin (Furch et al., 1999; Onishi et al., 1998). These experimental findings suggest that the formation of ionic bonds between Arg238 and Glu459 is essential for the initiation of ATP hydrolysis. We speculated the roles of Arg238 and Glu459 as follows: when ATP and myosin combine, a water molecule is trapped near the $\gamma$-phosphate of the ATPase pocket, and this triggers the formation of ionic bonds between Arg238 and Glu459 by electrostatic interactions. As a consequence, the ATP hydrolysis reaction starts without any influence of bulk water molecules. Therefore, Arg238 and Glu459 play roles in the capture of a lytic water molecule from numerous solvent water molecules and in the supply of a lytic water

molecule into the ATPase pocket by closing the gate of the ATPase pocket.

## CONCLUSION

Our QM calculation revealed that the mechanism of ATP hydrolysis by myosin is a single-elementary reaction with Walden inversion of γ-phosphate, and QM and MD calculations suggested that there is an effect of amino acid residues in the ATPase pocket. Lys185 plays a role in maintaining the appropriate structure of phosphate groups in the nucleotide. Thr186 and Ser237 maintain the conformation of the phosphates of the nucleotide through the $Mg^{2+}$ ion. Arg238 and Glu459 play roles in keeping a lytic water molecule at the appropriate position for initiating the hydrolysis.

This work was supported in part by the super computer Vpp700e in Institute of Physical and Chemical Research (RIKEN). The authors thank the Research Center for Computational Science, Okazaki. The computations were also carried out by the DRIA System at the Faculty of Pharmaceutical Sciences, Chiba University.

## REFERENCES

Abola, E. E., F. C. Bernstein, S. H. Bryant, T. F. Koetzle, and J. Weng. 1987. Protein Data Bank. *In* Allen FH, Bergerhoff G, Sievers R, editors. Crystallographic Database: Information of the International Union of Crystallography. Bonn, Data Commission of the International Union of Crystallography. 107–132.

Abola, E. E., N. O. Manning, J. Prilusky, D. R. Stampf, and J. L. Sussman. 1996. The Protein Data Bank: current status and future challenge. *J. Res. Natl. Inst. Stand. Technol.* 101:231–241.

Bagshaw, C. R., J. F. Eccleston, F. Eckstein, R. S. Goody, H. Gutfreund, and D. R. Trentham. 1974. The magnesium ion-dependent adenosine triphosphatase of myosin. Two-step processes of adenosine triphosphate association and adenosine diphosphate dissociation. *Biochem. J.* 141: 351–364.

Becke, A. D. 1993. Density-functional thermochemistry. III. The role of exact exchange. *J. Chem. Phys.* 98:5648–5652.

Berendsen, H. J., J. P. Postma, W. F. van Gunsteren, A. DiNola, and J. R. Haak. 1984. Molecular dynamics with coupling to an external bath. *J. Chem. Phys.* 81:3684–3690.

Bernstein, F. C., T. F. Koetzle, G. J. Williams, E. F. Meyer, M. D. Brice, Jr., J. R. Rodgers, O. Kennard, T. Shimanouchi, and M. Tasumi. 1977. The Protein Data Bank: a computer-based archival file for macromolecular structure. *J. Mol. Biol.* 112:535–542.

Cornell, W. D., P. Cieplak, C. I. Bayly, I. R. Gould, K. M. Merz Jr., D. M. Ferguson, D. C. Spellmeyer, T. Fox, J. W. Caldwell, and P. A. Kollman. 1995. A second-generation force field for the simulation of proteins and nucleic acids. *J. Am. Chem. Soc.* 117:5179–5197.

Fisher, A. J., C. A. Smith, J. B. Thoden, R. Smith, K. Sutoh, H. M. Holden, and I. Rayment. 1995. X-ray structures of the myosin motor domain of *Dictyostelium discoideum* complexed with MgADP.BeFx and MgADP.AlF4-. *Biochemistry.* 34:8960–8972.

Frisch, M. J., G. W. Trucks, H. B. Schlegel, M. A. Robb, J. R. Cheeseman, V. G. Zakrzewski, J. A. Montgomery, R. E. Stratmann, J. C. Burant, S. Dapprich, J. M. Millan, A. D. Daniel, K. N. Kudin, M. C. Strain, O. Farkas, J. Tomasi, V. Barone, M. Cossi, R. Cammi, B. Mennucci, C. Pomelli, S. Clifford, J. Ochterski, G. A. Petersson, P. Y. Ayala, Q. Cui, K. Morlkuma, D. K. Malick, A. D. Robuck, K. Raghavachari, J. B. Foresman, J. Cioslowski, J. V. Oritiz, A. G. Baboul, B. B. Stefanov, G. Liu, A. Liashenko, P. Piskorz, I. Komaromi, R. Gomperts, R. L. Martin, D. J. Fox, T. Keith, M. Al-Laham, C. Y. Peng, A. Nanayakkara, C. Gonzalez, M. Challacombe, C. Gill, M. Head-Gordon, E. S. Replogle, and J. A. Pople. Gaussian 98, Revision A.7. Pittsburgh, PA, Gaussian, Inc., 1998.

Furch, M., S. Fujita-Becker, M. A. Greeves, K. C. Holmes, and D. J. Manstein. 1999. Role of the salt-bridge between switch-1 and switch-2 of *Dictyostelium* myosin. *J. Mol. Biol.* 290:797–809.

Gulick, A. M., C. B. Bauer, J. B. Thoden, and I. Rayment. 1997. X-ray structure of the MgADP, Mg ATPγS, and MgAMPPNP complexes of the *Dictyostelium discoideum* myosin motor domain. *Biochemistry.* 36: 11619–11628.

Jorgensen, W. L., J. Chandrasekhar, and J. D. Madura. 1983. Comparison of simple potential functions for simulating liquid water. *J. Chem. Phys.* 79:926–935.

Lee, C., W. Yang, and R. G. Parr. 1988. Development of the Colle-Salvetti correlation-energy formula into a functional of the electron density. *Phys. Review B.* 37:785–789.

Li, X. D., T. E. Rhodes, R. Ikebe, T. Kambara, H. D. White, and M. Ikebe. 1998. Effects of mutations in the γ-phosphate binding site of myosin on its motor function. *J. Biol. Chem.* 273:27404–27411.

Miehlich, B., A. Savin, H. Stoll, and H. Preuss. 1989. Results obtained with the correlation energy density functionals of Becke and Lee, Yang and Parr. *Chem. Phys. Lett.* 157:200.

Onishi, H., M. F. Morales, S. Kojima, K. Katoh, and K. Fujiwara. 1998. Smooth muscle myosin. Amino acid residues responsible for the hydrolysis of ATP. *Adv. Exp. Med. Biol.* 453:99–104.

Pearlman, D. A., D. A. Case, J. W. Caldwell, W. S. Ross, T. E. Cheatham III, S. DeBolt, D. Ferguson, G. Seibel, and P. A. Kollman. 1995. AMBER, a package of computer programs for applying molecular mechanics, normal mode analysis, molecular dynamics and free energy calculations to simulate the structural and energetic properties of molecules. *Comp. Phys. Commun.* 91:1–41.

Rayment, I., W. R. Rypniewski, K. Schmidt-Base, R. Smith, D. R. Tomchick, M. M. Benning, D. A. Winkelmann, G. Wesenberg, and H. M. Holden. 1993. Three-dimensional structure of myosin subfragment-1: a molecular motor. *Science.* 261:50–58.

Ryckaert, J. P., G. Ciccotti, and H. J. Berendsen. 1977. Numerical integration of the Cartesian equations of proteins and nucleic acids. *J. Comput. Phys.* 23:327–341.

Sasaki, N., and K. Sutoh. 1998. Structure-mutation analysis of the ATPase site of *Dictyostelium discoideum* myosin II. *Adv. Biophys.* 35:1–24.

Smith, C. A., and I. Rayment. 1996. X-ray structure of the magnesium(II). ADP. vanadate complex of the. *Dictyostelium discoideum* myosin motor domain to 1.9 Å. resolution. *Biochemistry*. 35:5404–5417.

Szabo, A., and N. S. Ostlund. 1989. Modern Quantum Chemistry: Introduction to Advanced Electronic Theory. New York, McGraw-Hill Publishing Co.